Organic Process Research & Development **2006**, *10,* 51–63

Hydrogenation of Plant Sterols over a Polymer Fiber-Supported Pd Catalyst

Jarkko Helminen*

Fermion Oy, Orion Group, P.O. Box 28, FIN-02101 Espoo, Finland

Erkki Paatero

Laboratory of Industrial Chemistry, Lappeenranta University of Technology, P.O. Box 20, FIN-53851 Lappeenranta, Finland

Ulf Hotanen

UPM-Kymmene Corporation, Kaukas Research Center, FIN-53200 Lappeenranta, Finland

Abstract:

The hydrogenation of a wood-based plant sterol mixture consisting of β-sitosterol, β-sitostanol, campesterol, and campestanol was studied using a polymer fiber-supported Pd catalyst. The effect of the operating variables was screened by a fractional factorial experimental design. The hydrogenation experiments revealed that the fiber catalyst is stable, that is metal species are not leached into the reaction mixture, and mechanical agitation does not damage the catalyst. Kinetic experiments were carried out at temperatures of 333−353 K at constant hydrogen pressure. The catalyst was observed to be very selective: the obtained β-sitostanol is a stereochemically pure α-form, and only three byproducts could be quantitatively detected for kinetic modeling. A power-law model and 12 mechanistic models based on two different mechanisms were fitted to the experimental data. The best model assumes the competitive adsorption of sterol and hydrogen molecules as well as the molecular hydrogen adsorption. This model is based on the direct hydrogenation of sterols to stanols without the formation of half-hydrogenated intermediates. The scale-up of hydrogenation process was successfully carried out in pilot-plant and industrial reactors.

Introduction

The economic importance of plant sterols, especially wood-based sterols, has grown since Benecol margarine was introduced (Raisio Group plc., Finland). Clinical tests have shown that Benecol margarine decreases the cholesterol level of serum. The effective component of Benecol is β-sitostanol, i.e., the hydrogenated form of β-sitosterol, which has been produced at the Kaukas Chemical Mill since the 1980s. β-Sitostanol has been converted to a fat-soluble form by esterification with rape oil. The cholesterol-lowering effect of β-sitosterol was known already in the 1950s but because of its poor solubility in fats and water as a pure molecule its use remained minor before Raisio's invention. It has been later found that β-sitostanol lowers the cholesterol level more effectively than β-sitosterol.[1,2] Furthermore, β-sitostanol is resistant to oxidation, whereas β-sitosterol can be oxidized to harmful steroid compounds. Plant sterols also have a wide variety of other uses, e.g., in pharmaceuticals and cosmetics.[3,4]

Grafted polymer fibers have found applications in gas purifications.[5] Polymers, such as polyolefins and polystyrene, are irradiated by γ radiation or electron bombing; thereafter, the polymer fibers are dipped in a solution of acrylic acid or styrene. If styrene is used as the graft polymer, it has to be functionalized, e.g., by sulfonation. The poly(acrylic acid) grafted polyolefin fibers require no further functionalization, and they can be converted to a palladium form by ion exchange using a salt solution. This technique has been introduced for fiber catalyst manufacturing by Smoptech Ltd. (Johnson Matthey),[6] and it enables the production of the catalyst in the quantities required in fine chemical and pharmaceutical hydrogenation. The ion-exchanged palladium of fiber catalyst can be readily reduced by hydrogen under mild conditions. When Pd ions are reduced to the zerovalent state, they migrate over the surface to form aggregates. Hence, the polymer fiber-supported catalyst is an interesting combination of new and old features. On one hand, the catalytic activity of the fiber catalyst generates the aggregates of metal atoms, which is the most common form of supported metal catalysts. On the other hand, the polymer support of fiber catalyst is much more hydrophilic than the supports of conventional catalysts used in hydrogenation, since about 80% of the grafted acrylic acid groups are free.

This contribution deals with the hydrogenation of a wood-based plant sterol mixture using a polymer fiber-supported Pd catalyst. Because the fiber catalyst is very different from conventional catalysts and, to the best of our knowledge, only one detailed fiber catalyst hydrogenation study has been published,[7] it was necessary to investigate the effects of all

* Corresponding author. Telephone: +358 10 4294935. Fax: +358 10 4294597. E-mail: jarkko.helminen@orionpharma.com.

(1) Miettinen, T.; Vanhanen, H.; Wester, I. U.S. Patent 5,502,045, 1996.
(2) Miettinen, T.; Vanhanen, H.; Wester, I. U.S. Patent 5,958,913, 1999.
(3) Hamunen, A. U.S. Patent 4,420,427, 1983.
(4) Hamunen, A. U.S. Patent 4,422,974, 1983.
(5) Okamoto, J.; Sugo, T.; Fujiwara, K.; Sekigichi, H. *Radiat. Phys. Chem.* **1990**, *35*, 113−116.
(6) Näsman, J. H.; Ekman, K. B.; Sundell, M. J. U.S. Patent 5,326,825, 1993.
(7) Aumo, J.; Lilja, J.; Mäki-Arvela, P.; Salmi, T.; Sundell, M.; Vainio, H.; Murzin, D. Y. *Catal. Lett.* **2002**, *84*, 219−224.

10.1021/op050142j CCC: $33.50
Published on Web 12/09/2005

Table 1. **Investigated factors and their levels**

factor			low level (−)	high level (+)
1	total pressure	p (bar)	1	3
2	temperature	T (K)	333	353
3	agitation speed	N (min^{-1})	200	600
4	catalyst concentration[a]	$c_{Pd,st}$ (%)	0.1	0.5
5	sterol concentration[b]	c_{st} (%)	10	15
6	Pd concentration of catalyst	$c_{Pd,c}$ (%)	5	10
7	water concentration of sterol	$c_{H2O,st}$ (%)	1	3
8	water concentration of solvent	$c_{H2O,solv}$ (%)	0	5
9	water concentration of catalyst	$c_{H2O,c}$ (%)	0	60
10	solvent		IPA	NPA
11	sterol grade		A (c_S = 115 ppm)	B (c_S = 130 ppm)

[a] Calculated as the Pd concentration with respect to the amount of sterols in a reaction mixture. [b] Calculated from the total amount of solvent and sterols in a reaction mixture.

possible variables on the hydrogenation. Therefore, the first goal was to screen for the important operating variables by using a fractional factorial experimental design known as the Taguchi L_{12} matrix.[8] Then kinetic experiments were carried out, and the data were fitted to a power-law kinetic model and kinetic models based on different hydrogenation mechanisms. Finally, the sterol hydrogenations were performed in DIN250L and DIN4000L reactors.

2. Screening of Operating Variables

Fractional factorial designs are most often used in experimental situations to screen the effect of different variables, but they are also used for optimization. The simplest fractional factorial designs are known as Taguchi design matrixes.[8] For example, a Taguchi L_{12} matrix involves only 12 experiments, which is a reduced 2^{11} design. Consequently, only the main effects of 11 factors can be obtained using such a design, and the interactions are confounded with all the main effects.

The effects of 11 factors on the process performance of plant sterol hydrogenation were studied in this work using a Taguchi L_{12} design matrix. The factors were pressure, reaction temperature, agitation speed, catalyst concentration, substrate (sterol) concentration, Pd concentration of the catalyst, water concentration of the sterol mixture, water concentration of the solvent, water concentration of the catalyst, type of solvent, and sterol grade (Table 1). These factors were chosen since they were, based on some preliminary experiments thought to affect hydrogenation. The effect of some factors, such as pressure, is clear, but they were included to compare the magnitude of effect on the previously unknown factors. Additionally, some factors were excluded, since they could not be experimentally varied or they were not important. These factors were reaction time (2 h), grafting degree of the fiber catalyst, the material of the polymer support (polyethylene), and fiber length (5 mm). The levels of factors were chosen on the basis of a priori knowledge. The responses to the factors were the conversion of β-sitosterol, the yield of β-sitostanol, and the sulfur concentration of the catalyst after an experiment. Conversion and yield were natural choices as responses, since the former depicts the progress and the latter the selectivity of the reaction. On the basis of preliminary experiments that showed that the sterol mixture contained trace amounts of sulfur which deactivated the catalyst after a few times of use, the sulfur concentration of the catalyst was chosen as the third response. Thus, the goal was to find out the effect of operating conditions on the sulfur concentration of the catalyst.

3. Experimental Section

Hydrogenation experiments were conducted in a jacketed dead-end reactor system manufactured by Buchi (model BEP 280, V_R = 1000 cm^3). The pressure and temperature of the reactor were measured by Buchi P 203 and T202, respectively. A Lauda U3 with R400 controller was used for the temperature control within ±0.5 K. The reactor was equipped with a three-bladed turbine (47 mm diameter).

The three-phase hydrogenation of the plant sterol mixture was studied over a commercial polymer fiber-supported Pd catalyst (Smoptech Ltd., Finland). The catalyst support was a poly(acrylic acid) grafted polyethylene fiber (Pd concentration of 5 and 10%). Two different wood-based sterol mixtures (Kaukas Chemical Mill) were used in the experiments. Grade A contained 12.5% β-sitostanol, 77.4% β-sitosterol, 0.7% campestanol, and 6.7% campesterol. Grade B had the following composition: 11.9% β-sitostanol, 78.6% β-sitosterol, 0.6% campestanol, and 6.4% campesterol. Both sterol mixtures also contained traces of terpenoids, α-sitosterol, and sulfur (Table 1).

A Varian gas chromatograph 3400 Star series, equipped with a flame ionization detector, was used for the sterol analysis. The silylated compounds were separated in a 30 m × 0.32 mm glass capillary column DB-1, with a film thickness of 0.25 μm (J&W Scientific). The carrier gas was helium (υ_{He} = 2.0 cm^3 min^{-1}), and the split ratio was 1:30 (v_{H2} = 30 cm^3 min^{-1} and v_{air} = 300 cm^3 min^{-1}). The column was isothermal at 543 K, and the detector and injector temperatures were both set at 573 K. Retention times for the silylated sterols and aliphatic impurities were as follows: 8.44 min β-sitosterol, 8.66 min β-sitostanol, 7.09 min campesterol, 7.23 min campestanol, 8.05 min 7-sitosterol, 4.98 min sitostane, and 4.69 min sitostene.

(8) Taguchi, G. *System of Experimental Design: Engineering Methods to Optimize Quality and Minimize Costs*; UNIPUB/Kraus International Publications: New York, 1987; Vol. 1 and 2.

Scheme 1

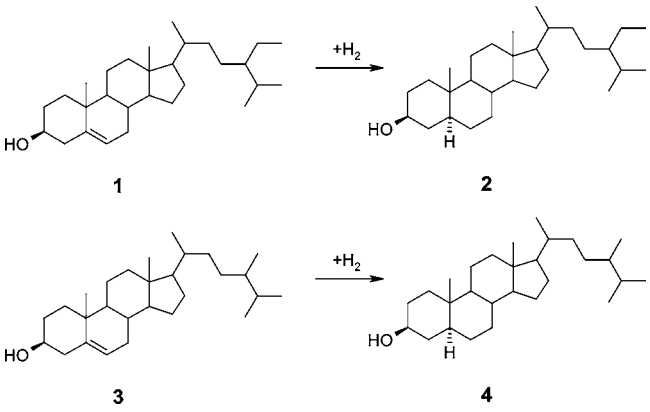

The water concentration of the solvent was determined by standard Karl Fischer titration. A Karl Fischer titration method presented for polymer matrixes was applied to the titration of the water concentration in the catalyst.[9] Determination of the catalyst sulfur concentration was done using a bomb method. The sulfur in a sample (ground, about 0.5 g) was first converted to a sulfate form by burning under pure oxygen at 30 atm in a closed bomb calorimeter, where about 1 mL of water was added to absorb sulfur dioxide. The sulfate concentration of water was analyzed using a standard ion-chromatography method.

4. Main and Side Reactions

In the hydrogenation of a commercial wood-based sterol mixture, the main reactions are the hydrogenation of β-sitosterol **1** to β-sitostanol **2** and campesterol **3** to campestanol **4** (Scheme 1).

Hydrogenation products were analyzed by mass spectroscopy and NMR. Contrary to preconceptions, the fiber catalyst was highly stereoselective, that is hydrogen was attached to the α-position of C5 (see Scheme 1). The α-side of a planar steroid molecule is below the plane. Since the polymeric catalyst support is not hydrophobic as are activated carbon or charcoal and the polymer effects, such as microenvironmental interactions, coordination unsaturation, viscous diffusion effects, steric effects, site-separation effects, and local concentration effects, about which the literature warned, were not known,[10] it was thought that the free acrylic acid groups in the fiber catalyst might work in a way similar to that of acidic media or promoters enabling the formation of the 5β-form.[11] Furthermore, Augustine et al.[12] have found that in the hydrogenation of planar molecules, the presence of water in the reaction mixture favors the formation of stereochemically different products. It was, therefore, surprising that the obtained β-sitostanol was the pure α-form.

In addition to the main products above, several byproducts were detected, mostly sitostane **5**, sitostene **6**, and 7-sitosterol **7**. The formation of byproducts is depicted in Scheme 2. Some other minor byproducts were also detected, but it was impossible to observe any trends required for kinetic modeling. If the concentrations of β-sitosterol, β-sitostanol, campesterol, campestanol, sitostane, sitostene, and 7-sitosterol are summed up, they compose, on average, 98.6% of the composition of the reaction mixture.

Scheme 2

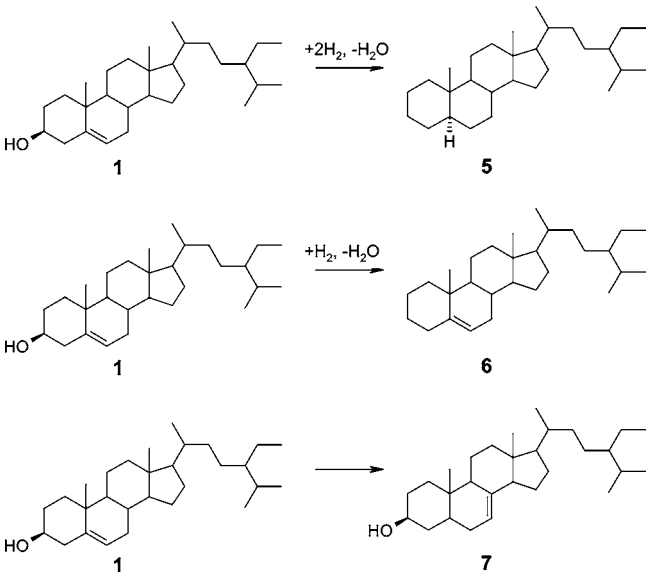

5. Kinetic Models

5.1. Mechanistic Models. Preliminary modeling implied that the most descriptive models are obtained when the rate-determining steps are surface reactions. Therefore, mechanisms based on adsorption and desorption steps being rate determining were abandoned. The following assumptions are made in the derivation of hydrogenation mechanisms and models: (1) the hypothesis of Langmuir's theory is applied for the adsorption sites; (2) hydrogen and steroid compounds are adsorbed both noncompetitively and competitively (*s* denotes a site for steroid molecules, and * denotes a site for hydrogen); (3) hydrogen is adsorbed molecularly ($j = 1$) and atomically ($j = 2$); (4) steroid compounds are adsorbed molecularly; and (5) hydrogen addition and side reaction (isomerization and formation of sitostane and sitostene) steps are rate determining. From the above, several alternative models are derived which account for the noncompetitive and competitive adsorption of hydrogen molecules and steroid molecules as well as molecular hydrogen adsorption and atomic hydrogen adsorption. In the modeling work, the following abbreviations are used: **1** = SS, **2** = SSH_2, **3** = CS, **4** = CSH_2, **5** = SEH_2, **6** = SE, and **7** = 7SS.

The following total site balances depict the noncompetitive adsorption approach

$$\sum_{i}^{N} \theta_{S,i} + \theta_{v,s} = 1 \tag{1}$$

$$\theta_H + \theta_{v,*} = 1 \tag{2}$$

where the subscript *v*,* denotes a vacant site for hydrogen, *v*,*s* denotes a vacant site for steroid molecules and *S,i* represents SS, SSH_2, CS, CSH_2, 7SS, SE, and SEH_2. *N* is the total number of steroid compounds in the reaction system.

(9) Iborra, M.; Fité, C.; Cunill, F.; Izquierdo, J. F. *React. Polym.* **1993**, *21*, 65.
(10) Sherrington, D. C.; Hodge, P. *Synthesis and Separations Using Functional Polymers*; Wiley: Chichester, 1988.
(11) Augustine, R. L. *Org. React. Steroid. Chem.* **1972**, *18*, 111−144.
(12) Augustine, R. L.; Migliorini, D. C.; Foscante, R. E.; Sodano, C. S.; Sisbarro, M. J. *J. Org. Chem.* **1969**, *34*, 1074−1085.

Table 2. **Lumped rate equations for Mechanism I**

non-competitive adsorption	competitive adsorption
$j = 2$ (atomic hydrogen): Model A1 $j = 1$ (molecular hydrogen): Model A2	$j = 2$ (atomic hydrogen): Model A3 $j = 1$ (molecular hydrogen): Model A4
$R_1 = \frac{k_1 c_{SS} c_H}{(1 + K_{SS} c_{SS})(1 + (K_H c_H)^{1/j})^j}$	$R_1 = \frac{k_1 c_{SS} c_H}{(1 + (K_H c_H)^{1/j} + K_{SS} c_{SS})^{j+1}}$
$R_2 = \frac{k_2 c_{CS} c_H}{(1 + K_{CS} c_{CS})(1 + (K_H c_H)^{1/j})^j}$	$R_2 = \frac{k_2 c_{CS} c_H}{(1 + (K_H c_H)^{1/j} + K_{CS} c_{CS})^{j+1}}$
$R_3 = \frac{k_3 c_{SS} (c_H)^2}{(1 + K_{SS} c_{SS})(1 + (K_H c_H)^{1/j})^{2j}}$	$R_3 = \frac{k_3 c_{SS} (c_H)^2}{(1 + (K_H c_H)^{1/j} + K_{SS} c_{SS})^{2j+1}}$
$R_4 = \frac{k_4 c_{SS} c_H}{(1 + K_{SS} c_{SS})(1 + (K_H c_H)^{1/j})^j}$	$R_4 = \frac{k_4 c_{SS} c_H}{(1 + (K_H c_H)^{1/j} + K_{SS} c_{SS})^{j+1}}$
$R_5 = \frac{k_5 c_{SS}}{1 + K_{SS} c_{SS}}$	$R_5 = \frac{k_5 c_{SS}}{1 + (K_H c_H)^{1/j} + K_{SS} c_{SS}}$

In the competitive adsorption approach, it is assumed that the hydrogen and steroid molecules are adsorbed onto the same sites, which can be denoted as $\theta_v = \theta_{v,*} = \theta_{v,s}$. Thus, the total site balance for the competitive adsorption approach is expressed as

$$\theta_H + \sum_i^N \theta_{S,i} + \theta_v = 1 \tag{3}$$

5.1.1. Mechanism I. It is presumed in this mechanism that the products are formed directly from the reactants without the formation of any half-hydrogenated intermediates. The rate-determining steps are the surface reaction between adsorbed β-sitosterol and adsorbed hydrogen (RDS1), the surface reaction between adsorbed campesterol and adsorbed hydrogen (RDS2), the formation of sitostane (RDS3), the formation of sitostene (RDS4), and the isomerization reaction of β-sitosterol producing 7-sitosterol (RDS5). Consequently, the lumped rate equations of the rate-determining surface reaction steps for the noncompetitive and competitive adsorption approaches of Mechanism I are presented in Table 2.

5.1.2. Mechanism II. This mechanism is based on the Horiuti−Polanyi mechanism which contains a step for the formation of half-hydrogenated intermediates. The Horiuti−Polanyi mechanism is widely used to describe the hydrogenation of olefinic double bonds, including steroid compounds, in organic chemistry.[13] The rate-determining steps of Mechanism II are the addition of a second hydrogen atom to β-sitosterol (RDS1), the addition of second hydrogen atom to campesterol (RDS2), and the formation of sitostane either directly from β-sitosterol or from the half-hydrogenated intermediate (RDS3). The rate-determining steps 4 and 5 are equal to Mechanism 1. Table 3 shows the lumped rate equations of the rate-determining surface reaction steps for the noncompetitive and competitive adsorption approaches of Mechanism II.

(13) Augustine, R. L.; O'Hagan, P. J. *Chem. Ind.* **1990**, *40*, 111−136.

5.2. Power-Law Model. The simplest way to describe the hydrogenation kinetics is to use empirical power-law rate equation models. These models are simple to use, and they often give an accurate fit to experimental data; however, the lack of a thermodynamical basis limits their use in extrapolation.[14] The power-law model in the hydrogenation of a sterol mixture for a steroid compound k can be written as

$$R_k = k_k {c_H}^m {c_k}^n \tag{4}$$

where m and n are empirical exponents.

6. Reactor Model and Parameter Estimation Procedure

The generation rates of each component in the reaction mixture are obtained from the reaction rates R_1-R_5 and the stoichiometry

$$r_{SSH_2} = R_1 \tag{5}$$

$$r_{SS} = -R_1 - R_3 - R_4 - R_5 \tag{6}$$

$$r_{CSH_2} = R_2 \tag{7}$$

$$r_{CS} = -R_2 \tag{8}$$

$$r_{SEH_2} = R_3 \tag{9}$$

$$r_{SE} = R_4 \tag{10}$$

$$r_{7SS} = R_5 \tag{11}$$

Hydrogen concentration in the reaction mixture was estimated from Henry's law equation[15]

$$c_H = \frac{p_H c_t}{K} \tag{12}$$

where K is the Henry constant.

(14) Ramachandran, P. A.; Chaudhari, R. V. *Three-phase Catalytic Reactors*; Gordon and Breach: New York, 1983.

Table 3. **Lumped rate equations for Mechanism II (Horiuti−Polanyi)**

non-competitive adsorption	competitive adsorption
$j = 2$ (atomic hydrogen): Models B1 ($R_{3,1}$) and C1 ($R_{3,2}$) $j = 1$ (molecular hydrogen): Models B2 ($R_{3,1}$) and C2 ($R_{3,2}$)	$j = 2$ (atomic hydrogen): Models B3 ($R_{3,1}$) and C3 ($R_{3,2}$) $j = 1$ (molecular hydrogen): Models B4 ($R_{3,1}$) and C4 ($R_{3,2}$)
$R_1 = \dfrac{k_1 c_{SS}(c_H)^{2/j}}{(1 + K_{SS}c_{SS})(1 + (K_H c_H)^{1/j})^j}$	$R_1 = \dfrac{k_1 c_{SS}(c_H)^{2/j}}{(1 + (K_H c_H)^{1/j} + K_{SS}c_{SS})^2}$
$R_2 = \dfrac{k_2 c_{CS}(c_H)^{2/j}}{(1 + K_{CS}c_{CS})(1 + (K_H c_H)^{1/j})^j}$	$R_2 = \dfrac{k_2 c_{CS}(c_H)^{2/j}}{(1 + (K_H c_H)^{1/j} + K_{CS}c_{CS})^2}$
$R_{3,1} = \dfrac{k_3 c_{SS}(c_H)^2}{(1 + K_{SS}c_{SS})(1 + (K_H c_H)^{1/j})^{2j}}$	$R_{3,1} = \dfrac{k_3 c_{SS}(c_H)^2}{(1 + (K_H c_H)^{1/j} + K_{SS}c_{SS})^{2j+1}}$
$R_{3,2} = \dfrac{k_3 c_{SS}(c_H)^{4/j}}{(1 + K_{SS}c_{SS})(1 + (K_H c_H)^{1/j})^3}$	$R_{3,2} = \dfrac{k_3 c_{SS}(c_H)^{4/j}}{(1 + (K_H c_H)^{1/j} + K_{SS}c_{SS})^4}$
R_4 and R_5 are the same as in the mechanism I	

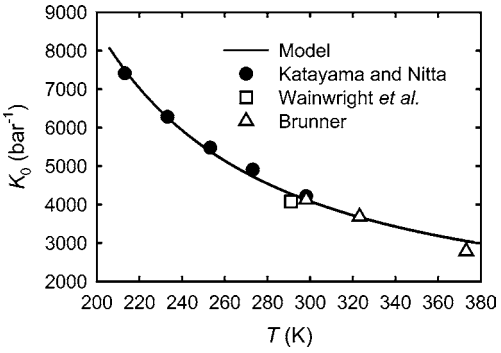

Figure 1. **Temperature dependence of the Henry law constant for hydrogen solubility in 1-propanol.**

For the temperature dependence of Henry's constant, a correlation containing all published hydrogen solubility data for 1-propanol could not be found in the literature.[16] Thus, from all the sources found,[15,17−20] the Henry constant values at different temperatures were combined and fitted to the van't Hoff equation[21]

$$K = K_0 \exp\left(\frac{-\Delta H_0}{RT}\right) \tag{13}$$

as shown in Figure 1.

Although the sterol concentration in the reaction mixture was 10 wt %, it is only about 1.6 mol %. Presumably, the effect of sterols on hydrogen solubility is low, and satisfactory estimates for hydrogen concentration can be obtained by these equations.

Attempts were made to study the influence of intraparticle diffusion through conducting hydrogenation experiments using a pulverized fiber catalyst. However, fibers do not withstand grinding, and the hydrogenation rates were lower than in the experiments where nonpulverized fibers were used. SEM analyses also revealed that the fibers were badly damaged in grinding. It is to be emphasized that the diameter of the catalyst fiber is 10 μm in dry form, but the fiber swells in solvent to about 20−30 μm.

The gas−liquid mass-transfer resistance and the external film resistance of the catalyst fiber were eliminated in the experiments using vigorous agitation. Therefore, the mass-transfer flux of hydrogen from the gas phase to the liquid phase is not needed in the semi-batch three-phase reactor model. Additionally, because the volume of liquid phase was presumed to be constant, the mass balance of liquid phase can then be used as the reactor model

$$\frac{dc_i}{dt} = r_i \frac{m_{cat}}{V_L} \tag{14}$$

where m_{cat} is the mass of catalyst in the reaction mixture.

Concentration data obtained from the hydrogenation experiments were fitted to the reactor model including the actual rate equations, generation rates, Arrhenius equation for the temperature dependence of the rate constants, hydrogen concentration equations, and 1-propanol vapor pressure correlation. The solution of the reactor model and the minimization of the object function were carried out by MODEST software.[22] Parameter estimation was performed for the 12 different mechanistic models and the power-law model for the concentration data simultaneously at temperatures of 333, 340, 346, and 353 K.

7. Results and Discussion

7.1. Screening Experiments. Table 4 shows the L_{12} fractional factorial design matrix and responses for each of

(15) Wainwright, M. S.; Ahn, T.; Trimm, D. L.; Cant, N. W. *J. Chem. Eng. Data* **1987**, *32*, 22−24.
(16) Fogg, P. G. T.; Gerrard, W. *Solubility of Gases in Liquids*; Wiley: Chichester, 1991.
(17) Katayama, T.; Nitta, T. *J. Chem. Eng. Data* **1976**, *21*, 194−196.
(18) Brunner, E. *Ber. Bunsen-Ges. Phys. Chem.* **1979**, *83*, 715−721.
(19) Clever, H. L. *Solubility Data Ser.* **1981**, *5−6*, 186.
(20) Young, C. L. *Solubility Data Ser.* **1981**, *5−6*, 441.
(21) Castellan, G. W. *Physical Chemistry*, 3rd ed.; ReAddison-Wesley: Reading (MA), 1983.
(22) Haario, H. *MODEST User's Manual*; ProfMath: Helsinki, 1994.

Table 4. **L_{12} design matrix and values of the responses**

	factors											responses		
exp	**1**	**2**	**3**	**4**	**5**	**6**	**7**	**8**	**9**	**10**	**11**	X (%)	Y (%)	$c_{S,c}$ (ppm)
1	−	−	−	−	−	−	−	−	−	−	−	16.4	100.0	240
2	−	−	−	−	−	+	+	+	+	+	+	18.1	95.3	310
3	−	−	+	+	+	−	−	−	+	+	+	68.4	86.4	150
4	−	+	−	+	+	−	+	+	−	−	+	13.1	74.4	150
5	−	+	+	−	+	+	−	+	−	+	−	42.6	92.9	670
6	−	+	+	+	−	+	+	−	+	−	−	98.8	89.2	180
7	+	−	+	+	−	−	+	+	−	+	−	98.1	94.8	100
8	+	−	+	−	+	+	+	−	−	−	+	18.2	99.5	130
9	+	−	−	+	+	+	−	+	+	−	−	29.5	89.0	240
10	+	+	+	−	−	−	−	+	+	−	+	70.9	97.9	620
11	+	+	−	+	−	+	−	−	−	+	+	67.7	91.1	140
12	+	+	−	−	+	−	+	−	+	+	−	42.0	94.0	210
Verf	+	+	+	+	−	+	−	−	+	+	−	98.8	95.6	–
Verf	+	+	+	+	−	+	−	−	+	+	−	98.6	94.6	–
Verf	+	+	+	+	−	+	−	−	+	+	−	98.7	95.3	–

Table 5. **. Values of effect % for all factors and responses**

factor		effect % (X)	effect % (Y)	effect % ($c_{S,c}$)
1	p (bar)	3.67	5.06	1.44
2	T (K)	5.75	12.79	13.64
3	N (min^{-1})	34.03	1.07	6.68
4	$c_{Pd,st}$ (%)	21.58	45.56	31.72
5	c_{st} (%)	18.79	18.43	0.03
6	$c_{Pd,c}$ (%)	0.89	0.06	0.85
7	$c_{H2O,st}$ (%)	0.04	3.62	20.47
8	$c_{H2O,solv}$ (%)	1.18	6.42	23.05
9	$c_{H2O,c}$ (%)	3.95	0.82	1.67
10	solvent	6.24	0.10	0.01
11	sterol grade	3.88	6.09	0.42

the 11 runs. Additionally, Table 4 contains the responses of the verification runs the meaning of which is explained below. The experiments of the L_{12} matrix were carried out in a randomized sequence to avoid bias. It must be emphasized that the effects of the factors cannot be determined in terms of the responses of any single run as presented in Table 4. Instead, the effects of each factor on conversion, yield, and sulfur concentration can be obtained from Table 5; it gives the average responses at the low and high levels of the factors.

Table 5 shows the effect % of each factor for the three responses. The effect % is the ratio of the pure sum of squares and the total sum of squares calculated in the analysis of variance,[8] and it describes the relative magnitude of effect for each factor. It can be seen from Table 5 that the agitation speed, catalyst concentration, and sterol concentration have the largest effect on the conversion of β-sitosterol. The difference in low and high level average responses, i.e., the effect on conversion, is 35.0%, −27.9%, and 26.0% for the agitation speed, catalyst concentration, and sterol concentration, respectively. The effect of hydrogen pressure, temperature, water concentration of the catalyst, solvent, and sterol grade on conversion is 11.5−15.0%. It is interesting to note that a slightly higher sulfur concentration of sterol grade B retards the hydrogenation rate. Also, the positive effect of the water concentration of the catalyst proves that the swelling of the fiber catalyst using water clearly improves the rate. Water in the reaction mixture generally has a negative effect on hydrogenation when the catalyst is hydrophilic. The hydrophilic catalyst is surrounded by water, and hydrophobic compounds, such as sterols, are not easily transferred to that phase. If the catalyst surface is hydrophobic, such as carbon, it would be vice versa.[23] In this work, the fiber catalyst is highly hydrophilic. Therefore, the negative effect of 6.5% for the water concentration of solvent agrees well with the literature above. The effect of Pd concentration of the catalyst and water concentration of the sterol mixture is lower than 5.7%, and thus their significance can be regarded as negligible.

The effects of factors on the yield of β-sitostanol are mainly negative, namely the effect of eight factors was negative (Table 5), whereas the effect of six factors on conversion was positive as above. Again, three factors (catalyst concentration (−10.1%), sterol concentration (−6.6%), and temperature (−5.5%)) affect yield more than the other factors. Surprisingly, the effect of pressure and agitation speed is positive but not as large as that of the catalyst concentration, sterol concentration, and temperature. It seems that the importance of hydrogen availability at the catalyst surface to the selectivity is less than that of the kinetic effects. The negative effect on yield has the water concentrations of the sterol mixture, solvent, and catalyst, whose magnitudes are 1.4−3.9%. The solvent grade and Pd concentration of the catalyst can be considered as insignificant factors, since the effect on yield was lower than 0.5%. It is seen from Table 5 that the catalyst concentration alone explains 45.56% of the variation in yield. If the effect % of temperature and sterol concentration is added to the value of the catalyst concentration, they explain altogether 76.68% of the variation of Y. The significance of other factors to the yield is, therefore, minor.

Table 5 reveals interesting features about the effect of the factors on the sulfur concentration of the fiber catalyst used in the hydrogenation of the plant sterol mixture. Four factors have a considerably larger effect on the sulfur concentration than the other factors. The catalyst concentration, water concentration of the solvent, water concentration of the sterol mixture, and temperature have values of −203, 173, −163, and 133 ppm, respectively. It is reasonable to assume that when the catalyst concentration increases the sulfur concentration of the catalyst decreases, because the sulfur amount remains constant in the reaction mixture. The effect of temperature on the sulfur concentration is also reasonable: the higher temperature accelerates the reactions of the sulfur compounds with the catalyst surface. In addition to temperature, the increasing water concentration of the solvent increases the sulfur concentration. This can be explained by the fact that the sulfur compounds are inorganic and dissolve more readily in the reaction mixture when the water concentration is higher. The inorganic sulfur compounds probably originate from the pulping process, but there are also sulfur compounds of plant origin. It is much more difficult to find an explanation for the negative effect of the water concentration in the sterol mixture which is probably due to analytical inaccuracy, since the water concentration in the

(23) Augustine, R. L.; Techasauvapak, P. *J. Mol. Catal.* **1994**, *87*, 95−105.

Table 6. **Experimental conditions in the kinetic experiments**

factor			kinetic region	constant pressure	variable pressure
1	reaction time	t (h)	1	2	2
2	hydrogen pressure	p_{H2} (bar)	2.9	2.9	0−2.9
3	temperature	T (K)	333	333−353	333−353
4	agitation speed	N (min^{-1})	300−800	600	600
5	catalyst concentration[a]	$c_{Pd,st}$ (%)	0.2	0.2	0.2
6	sterol concentration[b]	c_{st} (%)	10	10	10
7	Pd concentration of catalyst	$c_{Pd,c}$ (%)	10	10	10
8	water concentration of sterol	$c_{H2O,st}$ (%)	1	1	1
9	water concentration of solvent	$c_{H2O,solv}$ (%)	0	0	0
10	water concentration of catalyst	$c_{H2O,c}$ (%)	60	60	60
11	solvent		NPA	NPA	NPA
12	sterol grade		A	A	A

[a] Calculated as the Pd concentration with respect to the amount of sterols in a reaction mixture. [b] Calculated from the total amount of solvent and sterols in a reaction mixture.

sterol mixture is small. The catalyst concentration, water concentration of the solvent, water concentration of the sterol mixture, temperature, and agitation speed explain 95.6% of the total variation of the sulfur concentration (Table 5).

Three verification runs were carried out to confirm the optimum combination of the factors and to obtain an estimate for the error. The optimum combination of factors is as follows: pressure 3 bar; temperature 353 K; agitation speed 600 min^{-1}; catalyst concentration 0.5%; sterol concentration 10%; Pd concentration of catalyst 10%; water concentration of sterol 1%; water concentration of solvent 0%; water concentration of catalyst 60%; solvent 1-propanol; and sterol grade A. This is similar to the optimum combination of factors obtained for conversion in Table 5 except that 10% Pd concentration of catalyst was chosen instead of 5%. Its effect on conversion is, however, so small that the 10% catalyst can be reliably used. The results of the verification runs are presented in Table 4. On average, the values of conversion and yield are respectively 98.7% and 95.2%. Although the optimum combination of factors is obtained for conversion, it also gives a high value for yield. In fact, both the conversion and yield are higher in the verification runs than in the runs for the L_{12} design.

8.2. Kinetic Experiments at Constant H_2 Pressure. The results above revealed that the fiber catalyst adsorbs sulfur from the reaction mixture. Therefore, four successive hydrogenation runs were performed using the same catalyst to verify the effect of deactivation. The second hydrogenation run gave the same reaction rate as the first run, whereas in the third hydrogenation run, the reaction rate was about 8% lower. In the fourth run, the reaction rate was over 30% lower than in the first hydrogenation run. Consequently, it is very likely that the deactivation has no effect during the first hydrogenation run with a fresh catalyst.

A significant disadvantage in the use of a polymer-supported metal catalyst has generally been the leaching of metal species from the catalyst and powdering in a mechanically agitated reactor.[24] In the present work, the samples from the reaction mixture of several hydrogenation runs were analyzed by ICP technique, and no traces of palladium were detected. Also, the fibers were undamaged when inspected by microscope, and they were easily filtered from the reaction mixture.

The validity of the kinetic region, i.e., the agitation speed where the mass transfer resistances are absent, was studied by six successive hydrogenation runs at agitation speeds of 300, 400, 500, 600, 700, and 800 min^{-1}. Experimental conditions are given in Table 6 and, with a few exceptions, are similar to those in the verification runs of the screening experiments. It could be noticed that the agitation speed of 600 min^{-1} was sufficient to eliminate the external mass-transfer resistances.

Table 7 shows the estimated kinetic parameters and the statistical values depicting a goodness-of-fit for the models of Mechanism I. This mechanism is based on the assumption that hydrogenation proceeds directly without any half-

Table 7. **Regression results for models A1-A4 of Mechanism I**

	noncompetitive adsorption		competitive adsorption	
	atomic hydrogen Model A1	molecular hydrogen Model A2	atomic hydrogen Model A3	molecular hydrogen Model A4
R^2 (%)	99.75	99.75	99.75	99.75
total SS	61720	61720	61720	61720
RSS	152.8	155.4	153.3	153.1
std. err. of estimate	0.9681	0.9763	0.9698	0.9691
$k_1(T_0)$	1.46 ± 2.79	1.13 ± 0.0844	1.77 ± 0.662	0.875 ± 0.0103
$E_{a,1}$ (kJ mol^{-1})	52.8 ± 2.46	53.1 ± 1.34	53.1 ± 1.44	52.0 ± 1.50
$k_2(T_0)$	1.51 ± 2.88	1.17 ± 0.0882	1.83 ± 0.699	0.912 ± 0.0647
$E_{a,2}$ (kJ mol^{-1})	36.7 ± 10.5	38.7 ± 10.4	37.4 ± 10.4	37.8 ± 10.4
$k_3(T_0)$	6.15 ± large[a]	3.73 ± 0.418	8.19 ± 5.10	2.41 ± 0.0255
$E_{a,3}$ (kJ mol^{-1})	36.4 ± 3.95	40.3 ± 0.886	35.1 ± 1.42	34.3 ± 0.862
$k_4(T_0) \times 10^3$	15.0 ± 28.7	11.8 ± 0.876	18.4 ± 6.87	9.05 ± 0.146
$E_{a,4}$ (kJ mol^{-1})	19.4 ± 2.65	33.6 ± 1.78	23.7 ± 1.98	20.9 ± 1.91
$k_5(T_0) \times 10^6$	68.4 ± 11.6	68.7 ± 13.3	178 ± 22.3	148 ± 2.18
$E_{a,5}$ (kJ mol^{-1})	44.6 ± 1.53	36.3 ± 1.60	44.0 ± 1.61	43.9 ± 2.10
K_H (dm^3 mol^{-1})	10.3 ± large[a]	35.9 ± 5.89	8.33 ± 9.64	3.55 ± 0.306
K_{SS} (dm^3 mol^{-1})	2.38 ± 0.514	2.26 ± 0.554	0.866 ± 0.0264	(1.11 ± 5.92) × 10^{-3}

[a] Large confidence interval refers to values of estimated relative standard errors >200%.

Table 8. **Correlation matrix for the parameters of model A4**

	$k_1(T_0)$	$k_2(T_0)$	$k_3(T_0)$	$k_4(T_0)$	$k_5(T_0)$	$E_{a,1}$	$E_{a,2}$	$E_{a,3}$	$E_{a,4}$	$E_{a,5}$	K_H	K_{SS}
$k_1(T_0)$	1											
$k_2(T_0)$	−0.431	1										
$k_3(T_0)$	0.63	−0.759	1									
$k_4(T_0)$	0.469	−0.301	0.448	1								
$k_5(T_0)$	0.386	−0.135	0.175	0.248	1							
$E_{a,1}$	0.253	−0.057	0.139	0.022	−0.137	1						
$E_{a,2}$	−0.046	0.045	−0.036	−0.035	−0.053	0.034	1					
$E_{a,3}$	0.071	−0.056	−0.031	−0.028	−0.002	0.35	−0.003	1				
$E_{a,4}$	0.065	−0.035	0.095	0.201	−0.113	0.344	0.028	0.1	1			
$E_{a,5}$	−0.064	−0.059	0.055	−0.093	0.038	0.453	0.06	0.093	0.268	1		
K_H	0.558	−0.922	0.803	0.507	0.211	−0.015	−0.049	−0.241	0.048	−0.002	1	
K_{SS}	−0.19	−0.08	0.054	−0.171	−0.426	0.467	0.091	0.036	0.339	0.681	0.001	1

Table 9. **Regression results for Models B1−B4 of Mechanism II where the RDS3 is the formation of sitostane directly from *β*-sitosterol**

	noncompetitive adsorption		competitive adsorption	
	atomic hydrogen Model B1	molecular hydrogen Model B2	atomic hydrogen Model B3	molecular hydrogen Model B4
R^2 (%)	99.75	99.75	99.75	99.75
total SS	61720	61720	61720	61720
RSS	152.9	152.5	154.0	153.7
std. err. of estimate	0.9686	0.9674	0.9720	0.9709
$k_1(T_0)$	1.10 ± large[a]	87.6 ± 49.5	1.37 ± large[a]	88.2 ± 78.9
$E_{a,1}$ (kJ mol^{-1})	52.5 ± 3.12	49.6 ± 1.90	52.8 ± 2.42	49.8 ± 2.49
$k_2(T_0)$	1.14 ± large[a]	90.9 ± 51.8	1.41 ± large[a]	91.5 ± 82.0
$E_{a,2}$ (kJ mol^{-1})	36.8 ± 10.6	34.5 ± 10.4	37.2 ± 10.5	34.6 ± 10.5
$k_3(T_0)$	3.02 ± large[a]	26400 ± 44200	6.83 ± large[a]	28500 ± 50900
$E_{a,3}$ (kJ mol^{-1})	35.7 ± 4.04	29.8 ± 3.92	34.3 ± 3.83	28.5 ± 4.0
$k_4(T_0) \times 10^3$	11.4 ± large[a]	9.81 ± 5.55	20.5 ± large[a]	9.88 ± 8.83
$E_{a,4}$ (kJ mol^{-1})	22.6 ± 3.18	18.8 ± 2.21	19.9 ± 3.33	19.1 ± 2.68
$k_5(T_0) \times 10^6$	161.0 ± 7.74	161.0 ± 7.60	185.0 ± 188.0	156.0 ± 69.6
$E_{a,5}$ (kJ mol^{-1})	41.4 ± 1.55	44.6 ± 1.53	44.5 ± 1.83	44.7 ± 1.85
K_H (dm^3 mol^{-1})	2.37 ± large[a]	16.4 ± large[a]	8.81 ± large[a]	9.44 ± large[a]
K_{SS} (dm^3 mol^{-1})	2.36 ± 0.516	2.25 ± 0.50	1.28 ± 1.34	1.03 ± 0.514

[a] Large confidence interval refers to values of estimated relative standard errors >200%.

hydrogenated intermediates. The coefficient of determination (R^2) is the same for all models (99.75%), but the residual sum of squares (RSS) and the standard error of estimation can be used to distinguish the most accurate model. Model A1 assumes both the noncompetitive adsorption of components and atomic hydrogen adsorption. This model gives the lowest RSS and standard error of estimation values in Mechanism I. However, the confidence interval of the parameters and the correlation between the parameters are very high, which makes the model thermodynamically unreliable. For example, the errors of pre-exponential factors ($k_1(T_0) - k_2(T_0)$) vary between 17 and 200%. The RSS of model A2 with the molecular hydrogen adsorption is higher than in model A1, but the confidence intervals of the parameters are considerably lower, namely, between 7.4 and 19.4%. In Mechanism I, the competitive adsorption model A4 has a quite low RSS (153.1), and its confidence intervals are the lowest. The errors of all pre-exponential factors and adsorption coefficients are below 8.6%, and the highest estimated relative standard error is 27.5% for activation energies. Additionally, the correlations between the parameters are low, as Table 8 shows.

In Mechanism II based on the formation of half-hydrogenated intermediates, the R^2 values are also the same for all models (Tables 9 and 10). Model B2 fits the experimental data most accurately, for its RSS is 152.5 and the standard error of estimate is 0.9674 (Table 9). Model B2 assumes the noncompetitive adsorption of the components, molecular hydrogen adsorption, and the formation of sitostane directly from *β*-sitosterol. Although Model B2 has a lower RSS and standard error of estimate values than Model A4, the confidence intervals and correlation of Model B2 are much higher, for example the errors of pre-exponential factors range from 4.7 to 167.5%. Models B1, B3, and B4, which have a similar sitostane formation step to model B2, are statistically not as reliable as model B2. In contrast with models B1−B4, models C1−C4 describe the mechanism which accounts for the formation of sitostene via a half-hydrogenated intermediate. Models C1 and C2, which assume noncompetitive adsorption, have the same RSS values, i.e., 152.7, but the standard error of estimate for model C1 of atomic hydrogen adsorption is slightly smaller. However, the confidence intervals of model C2 are considerably smaller. For example, the errors of the pre-exponential

Table 10. **Regression results for models C1−C4 of Mechanism II where the RDS3 is the formation of sitostane via a half-hydrogenated intermediate**

	noncompetitive adsorption		competitive adsorption	
	atomic hydrogen Model C1	molecular hydrogen Model C2	atomic hydrogen Model C3	molecular hydrogen Model C4
R^2 (%)	99.75	99.75	99.75	99.75
total SS	61720	61720	61720	61720
RSS	152.7	152.7	155.6	153.6
std. err. of estimate	0.9679	0.9680	0.9769	0.9707
$k_1(T_0)$	1.10 ± 1.85	79.2 ± 61.3	1.10 ± 1.59	79.3 ± 75.6
$E_{a,1}$ (kJ mol^{-1})	52.5 ± 2.47	49.3 ± 2.50	52.7 ± 2.08	49.4 ± 2.71
$k_2(T_0)$	1.14 ± 1.91	81.8 ± 63.6	1.14 ± 1.64	82.2 ± 78.4
$E_{a,2}$ (kJ mol^{-1})	36.9 ± 10.5	34.3 ± 10.5	37.1 ± 10.5	34.3 ± 10.6
$k_3(T_0)$	3.51 ± large[a]	2.18 ± 3.37	1.69 × 10^{-3} ± large[a]	(0.694 ± 0.992) × 10^{-3}
$E_{a,3}$ (kJ mol^{-1})	35.0 ± 3.98	35.0 ± 4.06	39.7 ± 3.76	42.6 ± 3.38
$k_4(T_0) \times 10^3$	11.4 ± 19.0	8.93 ± 6.92	15.0 ± large[a]	8.93 ± 8.52
$E_{a,4}$ (kJ mol^{-1})	19.7 ± 2.66	22.0 ± 2.69	27.9 ± 2.82	21.6 ± 2.85
$k_5(T_0) \times 10^6$	163.0 ± 7.79	162.0 ± 1.88	166.0 ± 119.0	149.0 ± 70.8
$E_{a,5}$ (kJ mol^{-1})	44.4 ± 1.53	46.2 ± 1.52	43.6 ± 1.74	46.2 ± 1.92
K_H (dm^3 mol^{-1})	2.38 ± large[a]	6.22 ± large[a]	3.04 ± large[a]	3.69 ± large[a]
K_{SS} (dm^3 mol^{-1})	2.37 ± 0.514	2.22 ± 5.52 × 10^{-3}	1.09 ± 0.821	1.02 ± 0.548

[a] Large confidence interval refers to values of estimated relative standard errors more than 200%.

Table 11. **Regression results for the power-law model**

R^2 (%)	99.76	$k_4(T_0) \times 10^3$	10.5 ± 3.0
total SS	61720	$E_{a,4}$ (kJ mol^{-1})	21.6 ± 2.05
RSS	147.6	$k_5(T_0) \times 10^3$	3.08 ± 1.13
std. err. of estimate	0.9604	$E_{a,5}$ (kJ mol^{-1})	44.9 ± 1.65
$k_1(T_0)$	0.397 ± 0.0412	m_1 (−)	0.781 ± 0.0451
$E_{a,1}$ (kJ mol^{-1})	51.6 ± 1.37	m_2 (−)	1.39 ± 0.559
$k_2(T_0)$	4.14 ± large	m_3 (−)	1.28 ± 0.0577
$E_{a,2}$ (kJ mol^{-1})	40.1 ± 11.7	m_4 (−)	1.21 ± 0.132
$k_3(T_0) \times 10^3$	30.6 ± 3.79	m_5 (−)	2.52 ± 0.178
$E_{a,3}$ (kJ mol^{-1})	39.3 ± 0.974		

factors for the models C2 and C1 range 1.2−154.9% and 4.8−200%, respectively. The competitive adsorption models C3 and C4 have higher RSS values than model C3 and C4, but the confidence intervals of estimated parameters are not lower than model C2. Generally, the confidence intervals and correlation matrixes of model C1−C4 are higher than those of model A4.

Activation energies are of the same order of magnitude in all the mechanistic models studied, for example $E_{a,1}$ are between 49.3 and 53.1 kJ mol^{-1}. The confidence intervals of activation energies are low compared to the other parameter estimates.

The power-law model gives statistically the most accurate fit to the experimental data (Table 11). The statistical values of goodness-of-fit are better than for the mechanistic models, for example the R^2 value is 99.76% and RSS is 147.6. The confidence intervals of parameter estimates are also rather low. The error of $k_2(T_0)$ exceeds 200%, but the errors of other pre-exponential factors are 10.4−36.7%.

Figures 2−5 show the fit of models A2, A4, B2, and C1 and the power-law model at temperatures of 333−353 K. The mechanistic models predict equally the concentrations of β-sitostanol, β-sitosterol, campestanol, and campesterol at all temperatures. For byproducts, the fits of the mechanistic models at 333 and 340 K are equally good, but some differences can be seen at 346 and 353 K. Model A2 predicts higher concentrations for sitostene and sitostane and lower concentrations for 7-sitosterol the than other models. Model A4 gives lower concentrations for 7-sitosterol and higher concentrations for sitostane than models B2 and C1. The fit of the power-law model is the same as the fit of the mechanistic models for β-sitostanol and β-sitosterol, but it gives a more accurate fit for campesterol and campestanol. Although, the power-law model gives the statistically most accurate fit, it fails in predicting byproduct formation. By viewing the fits of both the mechanistic and power-law models, model A4 seems to fit the best, but the differences are, however, very small and within experimental error.

Table 12. **Experimental conditions in the pilot- and plant-scale hydrogenations**

			value	
factor			pilot	plant
1	total pressure	p (bar)	3.2	1.5 ± 0.5
2	temperature	T (K)	353 ± 5[c]	340 ± 3
3	agitation speed	N (min^{-1})	180	120
4	catalyst concentration[a]	$c_{Pd,st}$ (%)	0.22	0.27
5	sterol concentration[b]	c_{st} (%)	10	10
6	Pd concentration of catalyst	$c_{Pd,c}$ (%)	10	10
7	water concentration of sterol	$c_{H2O,st}$ (%)	1	1
8	water concentration of solvent	$c_{H2O,solv}$ (%)	4.3	0.5
9	water concentration of catalyst	$c_{H2O,c}$ (%)	67	0
10	solvent		NPA	NPA
11	sterol grade		A	A
	catalyst weight		1.0 (wet)	8.0 (dry)
	batch size		150 kg	3000 kg

[a] Calculated as the Pd concentration with respect to the amount of sterols in a reaction mixture. [b] Calculated from the total amount of solvent and sterols in a reaction mixture. [c] Hydrogen were introduced at 333 K, but in the pilot batch 2 it took 20 min longer to reach 353 K.

8.3. Experiments with Varying H_2 Pressure. Two experiments were performed at 333 and 346 K where the reactor was initially pressurized to 2.9 bar H_2 and the pressure decrease as a function of time was measured. Then the reactor model together with independently fitted kinetic

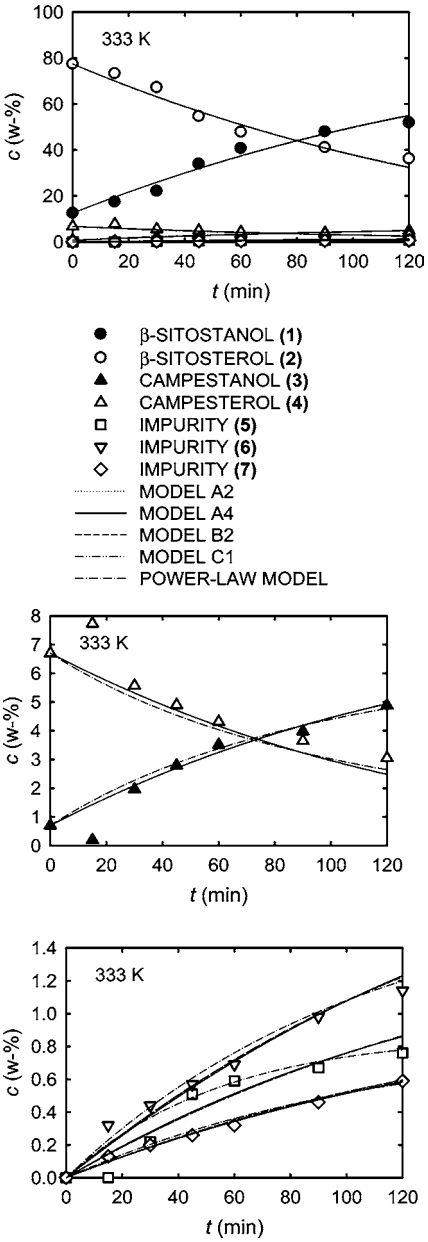

Figure 2. **Experimental (symbols) and predicted (curves) concentrations of steroid compounds in the hydrogenation of wood-based plant sterols at 333 K.**

models was used to predict the hydrogen consumption. Table 4 shows the experimental conditions in these two experiments. Figure 6 presents the comparison of experimental and simulated hydrogen pressures using the models A2, A4, B2, and C1. As we can see, model B2 does not satisfactorily predict the hydrogen pressures. All the other models in Mechanism II assuming molecularly adsorbed hydrogen showed similar behavior. These models can be regarded as equally inconsistent in predicting the hydrogenation of plant sterol with a polymer fiber-supported Pd catalyst. In general, this result is in agreement with the principles of Mechanism II, since the mechanism is based on the surface reaction of a half-hydrogenated intermediate with atomic hydrogen. Therefore, molecular hydrogen adsorption would be an irrational result. All the models of Mechanism I and the models assuming atomically adsorbed hydrogen of Mechanism II, such as models A2, A4, and C1 in Figure 6, predict much better the hydrogen consumption. The difference between these models is small, even if model A4 predicts the hydrogen consumption best. However, the predicted hydrogen pressures deviate considerably from the measured ones at low pressures. This can be caused by the inaccuracy of the hydrogen solubility model, especially at 333 K.

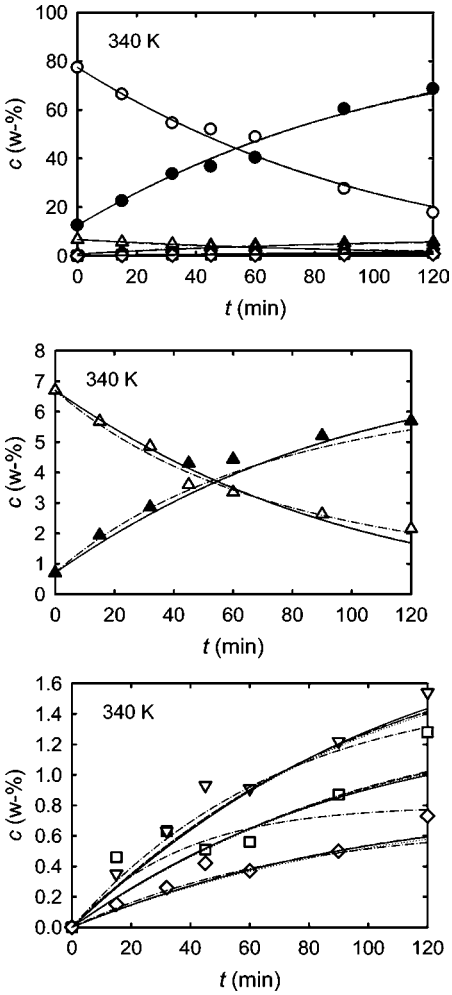

Figure 3. **Experimental (symbols) and predicted (curves) concentrations of steroid compounds in the hydrogenation of wood-based plant sterols at 340 K.**

The consistency of model A4 can be supported by previous findings. Augustine and co-workers have suggested that the catalyst surface consists of five different site types for olefinic hydrogenation: (1) $^{3}M_{I}$, $^{3}M_{R}$, and $^{3}M_{H}$ sites (corner or kink atoms) for the hydrogenation reaction, (2) ^{2}M isomerization site (edges or steps), and (3) ^{1}M hydrogen adsorption site (faces or terraces) which only adsorb hydrogen without taking part in the hydrogenation reaction.[13,23] Hence, in the present study, both sterols and hydrogen are adsorbed at the same sites, and then the competitive adsorption approach can be regarded as correct. The superiority of molecular hydrogen adsorption compared to atomic hydrogen adsorption can be explained with the aid of the following findings: when the metal aggregates are small (<1 nm), more than one hydrogen atom can adsorb on one metal atom on the surface. As mentioned above, the metal loading of the fiber catalyst has been carried out by ion exchange,

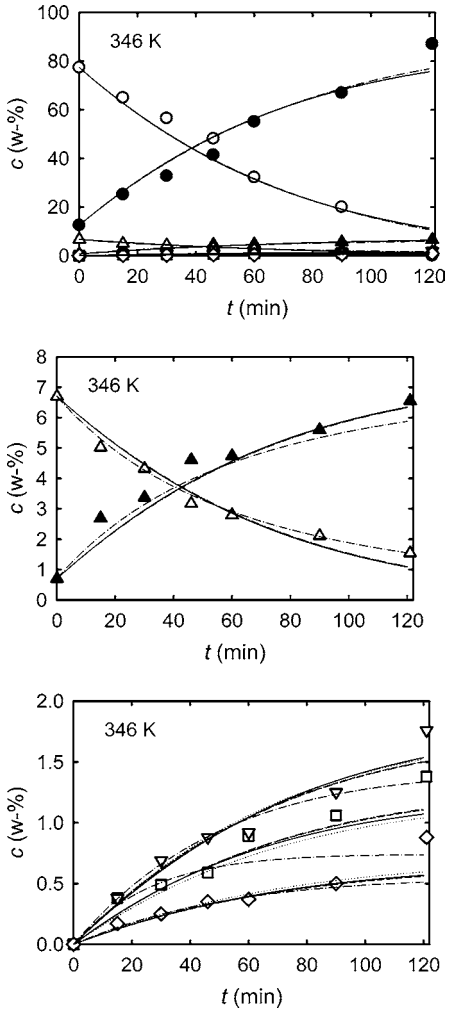

Figure 4. **Experimental (symbols) and predicted (curves) concentrations of steroid compounds in the hydrogenation of wood-based plant sterols at 346 K.**

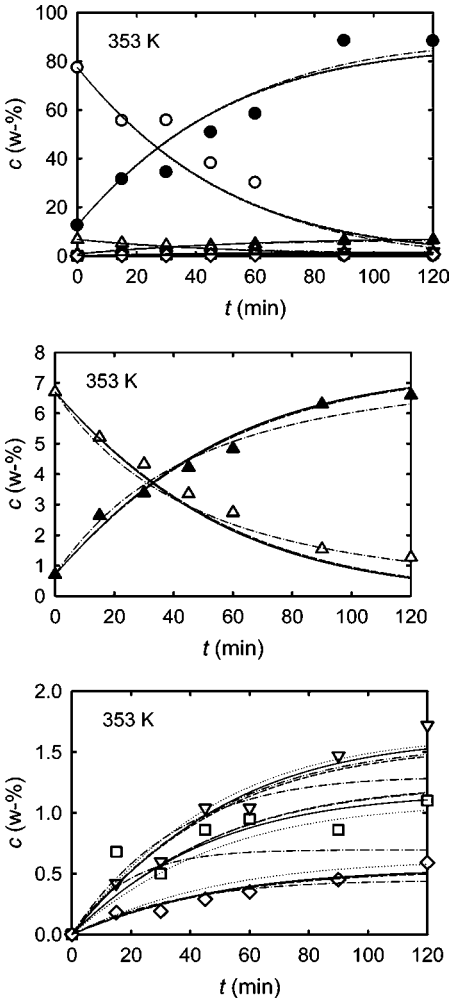

Figure 5. **Experimental (symbols) and predicted (curves) concentrations of steroid compounds in the hydrogenation of wood-based plant sterols at 353 K.**

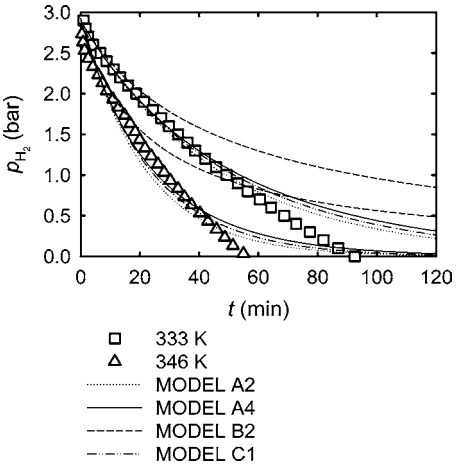

Figure 6. **Comparison between independently measured (symbols) and simulated (curves) hydrogen pressures in the gas-phase of laboratory reactor when after an initial pressurization the hydrogen feed was stopped.**

which is generally known to produce small metal aggregates.[24] The molecular hydrogen adsorption approach has been utilized a lot in the kinetic modeling of various hydrogenation reactions,[25] even though surface adsorption studies show that hydrogen is adsorbed atomically onto the hydrogenation catalyst metals.[26] Therefore, the molecular hydrogen adsorption in this work could mean, in fact, that two hydrogen atoms are adsorbed atomically to one site. This result is impossible to verify by hydrogen chemisorption experiments, since palladium is known to adsorb a large quantity of hydrogen in its crystal lattice.[27]

8.4. Scale-Up. Determination of reaction kinetics by laboratory experiments and kinetic modelling was essential in the process development and scale-up in a controlled way. We were able to calculate whether the chemical kinetics or gas−liquid mass transfer controls the hydrogenation rate in pilot and industrial scales. In this case, it was feasible to perform hydrogenations in glass-lined DIN vessels with poor agitation and low pressure. An expensive loop reactor was not necessary to use which reduced production costs. Pilot-scale hydrogenations were carried out in a glass-lined DIN250 L vessel and industrial-scale hydrogenations in a

(24) Gates, B. C. *Catalytic Chemistry*, 1st ed.; Wiley: New York, 1992.
(25) Jonker, G. H.; Veldsink, J.-W.; Beenackers, A. A. C. M. *Ind. Eng. Chem. Res.* **1997**, *36*, 1567−1579.
(26) Masel, R. I. *Principles of Adsorption and Reaction on Solid Surfaces*; Wiley: New York, 1996.
(27) Beenackers, A. A. C. M.; Van Swaaij, W. P. M. *Chem. Eng. Sci.* **1993**, *48*, 3109−3139.
(28) Cervený, L. *Chem. Eng. Commun.* **1989**, *83*, 31−63.

Table 13. **GC analysis of pilot- and plant-scale hydrogenations**

sampling time	**1** (%)	**2** (%)	**3** (%)	**4** (%)	**5** (%)	**6** (%)	**7** (%)
			pilot batch 1				
30 min	35.7	53.3	3.5	4.3	1.1	0.4	0.5
1 h	12.7	74.8	1.8	6.0	1.6	0.7	0.7
2 h	3.0	84.0	1.2	6.6	1.9	0.9	0.7
4 h 9 min	0.9	86.1	1.0	6.7	2.0	0.9	0.7
			pilot batch 2 (slow heating)				
30 min	51.0	38.0	4.8	3.1	0.7	0.3	0.5
1 h	31.1	56.6	3.2	4.6	1.3	0.7	0.6
2 h	10.4	77.2	1.7	6.2	1.7	1.1	0.6
4 h 30 min	1.5	84.4	1.0	6.9	2.0	1.3	0.5
			plant batch				
8 h	0.8	87.1	0.7	6.6	2.6	0.8	0.6

glass-lined DIN4000L vessel. Both reactors were equipped with a standard impeller and were heated by steam. Tables 12 and 13 show the experimental conditions and results of pilot- and plant-scale hydrogenations. We were not able to follow a similar heating profile for both pilot batches, and the hydrogenation rate was slower in the pilot batch 2 (Table 13). The plant batch was required to be carried out at 1.5 bar and 340 K, because the sealing allowed the pressure only up to 2 bar. In addition, a sampling without nitrogen purging was not possible in the plant reactor; thus, the samples were not taken during reaction. The experimental conditions of the plant batch led to a mild over-hydrogenation which can be seen in the higher amount of **5** as before. However, impurity **5** can be easily removed by crystallization. The most challenging problem in scale-up was the fiber catalyst recycling and regeneration. A regeneration method which allows the catalyst reuse in numerous batches could be later developed.

9. Conclusions

The hydrogenation of wood-based plant sterols, namely, β-sitosterol and campesterol, catalyzed by a polymer fiber-supported Pd catalyst was studied in the present work. The results revealed that the hydrogenation works well on a laboratory scale. Metal species are not leached into the reaction mixture, and mechanical agitation does not damage the fiber catalyst. A fractional factorial experimental design, known as the Taguchi L_{12} matrix, was used to screen the effects of 11 factors on the conversion of β-sitosterol, yield of β-sitostanol, and sulfur concentration of the catalyst. The agitation speed, catalyst concentration, and sterol concentration have the greatest effect on the conversion. A more interesting result, however, is that considerably higher conversions are obtained when the fiber catalyst is swelled with water compared to the use of dry catalyst fiber. The catalyst concentration, sterol concentration, and temperature affect the yield more than the other factors, e.g., agitation speed and pressure. Unquestionably, higher water concentration of solvent and higher temperature increase the catalyst sulfur concentration.

Kinetic experiments were carried out at temperatures of 333, 340, 346, and 353 K at a constant hydrogen pressure. Twelve mechanistic models and a power-law model were fitted to the experimental data. Statistical evaluation of the different models and fitted parameters showed that Model A4 is the best. This model is based on the mechanism where sterols are directly hydrogenated to stanols without the formation of half-hydrogenated intermediates. Moreover, the model assumes not only the competitive adsorption of hydrogen molecules and sterol molecules but also the molecular adsorption of hydrogen. Plant sterol hydrogenations with fiber catalyst were successfully carried out in pilot (250 L) and industrial (4000 L) scales.

Acknowledgment

Jarkko Helminen acknowledges the financial support of the Finnish Cultural Foundation and the Foundation of Lappeenranta University of Technology. We thank Smoptech Ltd. for supplying the catalyst.

NOTATION

c	concentration, % or mol dm^3
E_a	activation energy
k	rate constant
$k_k(T_0)$	pre-exponential factor
K	adsorption equilibrium constant
K_0	pre-exponential factor for the van't Hoff equation
m_{cat}	catalyst mass
p	pressure
r_k	generation rate
R_k	reaction rate
t	time
V_L	volume of liquid-phase
V_R	reactor volume
X	conversion of β-sitosterol
Y	yield of β-sitosterol
Greek Letters	
ΔH_0	enthalpy in the van't Hoff equation
q	surface coverage
Subscripts and Superscripts	
c	catalyst
CS	campesterol
CSH_2	campestanol
CSH	half-hydrogenated intermediate of campesterol

H	hydrogen
j	hydrogen atom index showing atomic or molecular adsorption, −
k	index of the rate determining step, −
m	exponent of hydrogen concentration in the power-law model
n	exponent of steroid compound concentration in the power-law model
N	total number of steroid compound in the reaction mixture
s	site for a steroid compound
S	sulfur
SE	sitostene
SEH_2	sitostane
S,i	*i*th steroid compound in the reaction mixture
solv	solvent
SS	β-sitosterol
SSH	half-hydrogenated intermediate of β-sitosterol
SSH_2	β-sitostanol
st	sterol
7SS	7-sitosterol
v	vacant site
*	site for hydrogen

Received for review August 9, 2005.

OP050142J